NeuroImage 90 (2014) 381–389

Contents lists available at ScienceDirect

NeuroImage

journal homepage: www.elsevier.com/locate/ynimg

An investigation into the functional and structural connectivity of the Default Mode Network

E.S.B. van Oort [a,b,c,*], A.M. van Cappellen van Walsum [a,b,c,d], D.G. Norris [a,b,c]

[a] Trigon building, Kapittelweg 29, 6525 EN Nijmegen, The Netherlands
[b] MIRA Institute for Biomedical Technology and Technical Medicine, University of Twente, The Netherlands
[c] Radboud University Nijmegen, Donders Center for Cognitive Neuroimaging, The Netherlands
[d] Department of Anatomy, Radboud UMC, The Netherlands

ARTICLE INFO

Article history:
Accepted 19 December 2013
Available online 29 December 2013

Keywords:
Resting state fMRI
Diffusion Weighted Imaging
Connectivity
Default Mode Network
Graph theory
Hubs

ABSTRACT

Connectivity analyses based on both resting-state (rs-)fMRI and diffusion weighted imaging studies suggest that the human brain contains regions that act as hubs for the entire brain, and that elements of the Default Mode Network (DMN) play a pivotal role in this network. In the present study, the detailed functional and structural connectivity of the DMN was investigated. Resting state fMRI (35 minute duration) and Diffusion Weighted Imaging (DWI) data (256 directions) were acquired from forty-seven healthy subjects at 3 T. Tractography was performed on the DWI data. The resting state data were analysed using a combination of Independent Component Analysis, partial correlation analysis and graph theory. This forms a data driven approach for examining the connectivity of the DMN. ICA defined regions of interest were used as a basis for a partial correlation analysis. The resulting partial correlation coefficients were used to compute graph theoretical measures. This was performed on a single subject basis, and combined to compute group results depicting the spatial distribution of betweenness centrality within the DMN. Hubs with high betweenness centrality were frequently found in association areas of the brain. This approach makes it possible to distinguish the hubs in the DMN as belonging to different anatomical association systems. The start and end points of the fibre tracts coincide with hubs found using the resting state analysis.

Introduction

Resting state functional MRI (rs-fMRI) has developed into a major tool for examining functional connectivity in the brain. In 1995, Biswal et al. showed the similarity between the functional activation map of a finger tapping experiment, and the correlation map to a seed placed inside that activation map (Biswal et al., 1995). Initially, this type of research generally followed the methods developed by Biswal et al., and used seed voxels and correlation maps (Fox and Raichle, 2007).

One resting state network (RSN) of particular interest is the Default Mode Network (DMN) (Buckner et al., 2008; Raichle et al., 2001). A meta-study of Positron Emission Tomography (PET) data found that regions of this network: the Medial Frontal Cortex (MFC), Inferior Parietal Lobule (IPL), Medial Temporal Lobe (MTL), and the Precuneus/Posterior Cingulate Cortex (Pc/PCC), show reduced metabolic activity during activation (Shulman et al., 1997). From a cognitive point of view, parts of the DMN are involved in processes such as episodic memory (Greicius et al., 2003, 2004). However, its higher activation during inactivity has seen it described as an important part of the idling mode of the brain (Raichle et al., 2001; Raichle and Snyder, 2007). Seed-based techniques are capable of detecting a number of RSNs, including the DMN (Cole et al., 2010). However, these methods include some bias in the form of the seed selection. This specificity to the seed voxel selection can be an advantage for some research questions (van den Heuvel and Hulshoff Pol, 2010). However, when searching for RSNs it becomes a disadvantage, because the resulting RSN map can be very sensitive to the location of the seed voxel (Cole et al., 2010). Exploratory data-driven techniques, like Independent Component Analysis (ICA) (Beckmann et al., 2005; Comon, 1994; Kiviniemi, 2003; McKeown et al., 1998) can avoid some of these disadvantages. Results obtained using ICA suggest that there are at least 10 large scale RSNs, having long range connections throughout the entire brain (Beckmann et al., 2005; Damoiseaux et al., 2006), and importantly, if sufficient data are acquired, higher order ICA can be used to detect more components (Kiviniemi et al., 2009).

In recent years graph theoretical measures have been introduced as a means of describing the network structure of the brain. These techniques have been applied both to resting state data (Salvador et al., 2005) and to fibre tracking data (Hagmann et al., 2008). Graph theory

* Corresponding author at: Trigon building, Kapittelweg 29, 6525 EN, Nijmegen, The Netherlands. Fax: +31 24 36 10652.
E-mail addresses: e.vanoort@fcdonders.ru.nl (E.S.B. van Oort), A.vanCappellenvanWalsum@anat.umcn.nl (A.M. van Cappellen van Walsum), david.norris@fcdonders.ru.nl (D.G. Norris).

1053-8119/$ – see front matter © 2013 Elsevier Inc. All rights reserved.
http://dx.doi.org/10.1016/j.neuroimage.2013.12.051

can be used to find hubs of connectivity, by identifying regions with high betweenness centrality. It has furthermore revealed that brain networks have a small world topography (Achard et al., 2006; Salvador et al., 2005; van den Heuvel et al., 2008b). Previous work on the graph theoretical structure of the brain using both resting state fMRI (van den Heuvel et al., 2008a) and fibre-tracking data (Hagmann et al., 2008; van den Heuvel et al., 2012) have identified the Pc/PCC region of the DMN as a major hub. This is in agreement with existing anatomical knowledge that parts of the Pc/PCC are so called Heteromodal Association Areas (HAAs), having many connections with other parts of the brain and being associated with advanced stages of information processing (Bassett et al., 2008). The unique role of HAAs is to bind multiple brain regions into distributed integrated networks (Achard et al., 2006; Mesulam, 1998; Nieuwenhuys et al., 2008).

The connectivity of the DMN has been investigated on the scale of the larger DMN regions. Fransson and Marrelec used partial correlation coefficients to investigate the large scale connectivity between regions of the DMN and found that the Pc/PCC region showed a heightened connectivity to other regions in the network (Fransson and Marrelec, 2008). Greicius et al. have previously investigated the use of both functional and anatomical connectivity of the DMN and showed that regions that have a high degree of functional connectivity are likely directly connected anatomically (Greicius et al., 2009), reflecting results previously obtained from other regions of the brain (Koch et al., 2002; Skudlarski et al., 2008). Van den Heuvel et al. investigated the link between this anatomical and functional connectivity and found that the DTI fibre path integrity of the cingulum tract is highly correlated with the functional connectivity of the regions it connects (van den Heuvel et al., 2008a). The present work expands on this previous literature, by performing a graph theoretical analysis of the functional connectivity pattern at a finer spatial scale than has hitherto been attempted, and relating this to the anatomical connectivity in the network. To this end, resting state fMRI data were obtained. These resting state data were used to perform single-subject ICA runs. The resulting regions were used for a detailed analysis of the organisation of the DMN, and to compute group averages and hubs of connectivity. High angular resolution Diffusion Weighted Imaging (DWI) data were also obtained in order to explore the relationship between the anatomical connectivity of the DMN using both deterministic and probabilistic tractography and its internal hub structure. Deterministic tractography provided a clear visualisation of the streamlines between regions, probabilistic tractography was added in order to verify the simpler method of deterministic tractography.

Methods

Subjects and data acquisition

Forty-seven subjects (age mean/std: 22.7/2.4, 24 male, 44 right handed) were scanned after giving informed written consent in accordance with the guidelines of the local ethics committee. All scans were acquired at 3 T on a Siemens Magnetom Trio system at the Donders Centre for Cognitive Neuroimaging. T1 anatomical, resting state fMRI and DWI data were acquired in one session. For the resting state scan, the scanner room was completely darkened. Lights were turned off and blinds pulled down. Subjects were instructed to relax, keep their eyes open, stay awake and try not to think about anything specific or dwell on one particular subject. Because this resting state scan was much longer than is usual, the subjects were monitored to ensure that they stayed awake. An infra-red camera normally used for eye tracking was used for this purpose.

Resting state fMRI data were acquired at 3 T using a Multi Echo - Echo Planar Imaging (ME-EPI) (Poser et al., 2006; Speck and Hennig, 1998) sequence with a Siemens 32 channel head coil. Voxel size was $3.5 \times 3.5 \times 3.5$ mm^3, flip angle = 80°, TR = 2000 ms, TEs = 6.9, 16.2, 25, 35 and 45 ms, matrix size 64×64, 39 slices, 1030 volumes, GRAPPA factor 3, 6/8 partial Fourier. Total scanning time for the resting state protocol was 35 min. The DWI protocol used the optimized acquisition order described by Cook et al. (2007). The DWI acquisition parameters were: voxel size $2.0 \times 2.0 \times 2.0$ mm^3, matrix size 110×110, TR = 13,000 ms, TE = 101 ms, 70 slices, 256 directions at b = 1500 s/mm^2 and 24 directions at b = 0. Finally, the T1 structural scan used an MPRAGE protocol, with acquisition parameters: voxel size $1.0 \times 1.0 \times 1.0$ mm^3, matrix size 256×256, 192 slices, TR = 2300 ms, TE = 3.03 ms, TI = 1100 ms, flip angle = 8°.

Preprocessing

rs-fMRI preprocessing was performed using Matlab scripts, and FSL's FEAT toolbox (fMRIB's Software Library, www.fmrib.ox.ac.uk/fsl). The multi-echo sequence that was used generates a volume for every echo at every time point. These echoes were combined as described by Poser et al. to allow the use of standard fMRI preprocessing tools (Poser et al., 2006). Of the 1030 combined volumes, the first six were discarded to allow the system to reach a steady state. Motion correction was performed prior to combining the multiple echoes using SPM5 functions (Wellcome Department of Imaging Neuroscience, University College London, UK). FEAT preprocessing involved the removal of non-brain regions using the Brain Extraction Tool (BET); 5 mm FWHM Gaussian spatial smoothing; spatial normalisation to Montreal Neurological Institute (MNI) space; a 0.01 Hz high pass filter, to remove low frequency scanner drifts; and ICA denoising. DWI preprocessing was performed with an in-house toolbox that corrects for artefacts induced by subject motion and cardiac pulsation (Zwiers, 2010). This toolbox uses a spatially informed tensor estimation technique that can robustly estimate the underlying tensor model from diffusion data that contains artefacts.

Analysis

Default Mode Network

Independent Component Analysis as implemented in FSL's MELODIC was applied to the time domain concatenated data of all subjects (Beckmann and Smith, 2004; Beckmann et al., 2005). This group analysis was set to obtain 30 components, with the DMN ending up as one component. The purpose of this analysis was to obtain a mask of the main regions of the DMN at the group level, for use in a detailed examination of the connectivity within this network.

ICA

The single subject resting state data were subsequently analysed using MELODIC. MELODIC was applied to the 4D Nifti files containing the preprocessed data, set to obtain 75 Independent Components (ICs) for each subject. The long measurement time, ICA denoising, and the large number of time points gives an increase in power, which makes this high number of components possible even at the single subject level. MELODIC was set to generate 75 ICs to keep the number of components manageable, though in principle more could have been generated by letting MELODIC determine by itself how many components to use (Beckmann et al., 2005). When this was tested, MELODIC found around 300 components per subject.

Parcellation

The single subject ICs related to functional anatomy were manually selected, and any components containing artefacts, white matter and regions outside of the brain were rejected. Regions within these components smaller than 100 voxels were removed to reduce clutter. The remaining components were masked with the DMN mask, and form the basis of the individual DMN parcellation. Each component was split into its constituent regions. Some of these regions overlapped with regions from other components. For the purposes of this work, the two regions that overlap will be called the parent regions. To

make sure that every voxel is assigned to only one region, these overlaps had to be resolved. This was accomplished using the following criteria (Fig. 1).

- In the case of a small (<100 voxels) overlap, each of the overlapping voxels was assigned to the parent region with which they have the highest temporal correlation.
- In the case of a large (>100 voxels) overlap, which takes up less than 85% of the voxels of both parents, the overlap is separated from its parents, and becomes a new region.
- In all other cases, the two parents get merged into one region.

This process was applied iteratively. To determine the order in which to resolve these overlaps, every combination of two overlapping regions was examined. They were ordered by calculating the percentage of voxels of each parent that are part of the overlap. The criteria stated above were applied to the combination of overlapping regions with the lowest value for this percentage. After this overlap was resolved using the criteria stated above, a different combination of overlapping regions had the smallest percentage of overlapping voxels, and so on. This process was repeated until there were no more overlapping regions present in the parcellation. The threshold value of 100 voxels was determined empirically. It resulted in a parcellation of the main DMN regions into smaller sub-regions with a high level of detail, but still a manageable number of ROIs for further analysis.

Partial correlations

The group level mask of the DMN was used to examine this network for detailed and localized connectivity between its main component regions, using both resting state correlations and DWI tractography. The parcellations of the DMN were used as ROIs for a partial correlation analysis, with the exceptions of the left and right hippocampi. Although the left and right hippocampi were present in the group ICA results, they were replaced with a segmentation for every subject using Freesurfer. These regions have a large variation in size and shape between subjects. The ICA would therefore find the voxels with the highest overlap. This means that if these main regions were used, a large number of voxels that are part of the hippocampus would be ignored. Using the single subject segmentation solves this problem, and should improve the results. This was only done for the hippocampi, because the other main DMN regions do not occupy a single anatomical region that can be readily segmented. The partial correlation analysis was created by adapting the method from Salvador et al. (2005) to use the sub-regions from the DMN parcellation instead of the Automatic Anatomical Labelling (AAL) template regions. Time courses for each ROI were obtained using a spatial regression as implemented in FSL. These time courses were used to estimate the partial correlation matrix for every subject. This matrix contains the Partial Correlation Coefficients (PCCs) for every combination of two ROIs.

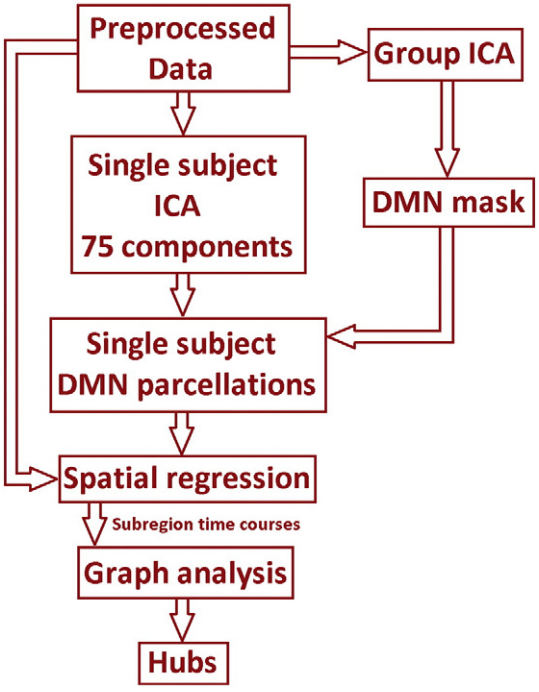

Fig. 1. Schematic representation of resting state analysis pipeline.

Network analysis

The PCCs between all the sub-regions of the complete parcellated DMN were used to create a single subject connectivity network. In this network, every sub-region forms a node. The PCCs were used to define weighted edges between the nodes. The resulting network makes it possible to obtain graph theoretical measures, such as node centrality. The node centrality was calculated using the Brain Connectivity Toolbox. For more details on the underlying graph methods, see (Rubinov and Sporns, 2010). This measure indicates the importance of the node in the topography of the network. The nodes with the largest betweenness centrality can be ascribed the role of hubs in the network. The locations of the ROIs that form the basis of every node is known, so the locations of the hubs are also known for every subject. This makes it possible to generate a map of the betweenness centrality for every voxel for each subject. By taking the average over all subjects, the average betweenness centrality of every voxel can be calculated. The regions with high betweenness centrality show main hubs of connectivity for the complete DMN. These methods make it possible to examine small-scale hubs within the DMN at the group level.

DWI — Deterministic fibre tracking

The deterministic fibre tracking was performed using the Camino software package (Cook et al., 2006). For this analysis, the combinations of Pc/PCC-MFC, Pc/PCC-left MTL and Pc/PCC-right MTL ROIs were used as seed/target regions. FSL was used to perform the linear and non-linear (co)registrations. First, the b = 0 diffusion scan was co-registered to the T1 anatomical scan. The T1 scans were first linearly and then non-linearly registered to the MNI152 T1 template using FLIRT and FNIRT from FSL. These two transformations were combined by Camino to form the single diffusion to MNI transformation. Camino was then used to: calculate the inverse of this transformation, and thus transform the ROIs from MNI space to diffusion space; and to perform deterministic Q-ball tractography in diffusion space (Tuch, 2004). The resulting tracts were transformed back into MNI space to compare them across subjects and to the resting state results.

DWI — Probabilistic tractography

Probabilistic tractography was performed using the FSL diffusion toolbox (Behrens et al., 2003, 2007). BEDPOSTX and PROBTRACKX were used to estimate diffusion parameters and generate probabilistic streamlines between the elements of the DMN. This analysis was performed twice: once with the Pc/PCC and once with the MFC as seed, and the other regions as targets. These results combined show the diffusion based connectivity between the MFC and the Pc/PCC.

Results

DMN regions

All subjects managed to stay awake for the total duration of the resting state scan. The data from all 47 subjects could be successfully processed and analysed. The 30 component group level ICA found the DMN as one component, which is shown in Fig. 2. These regions, with the

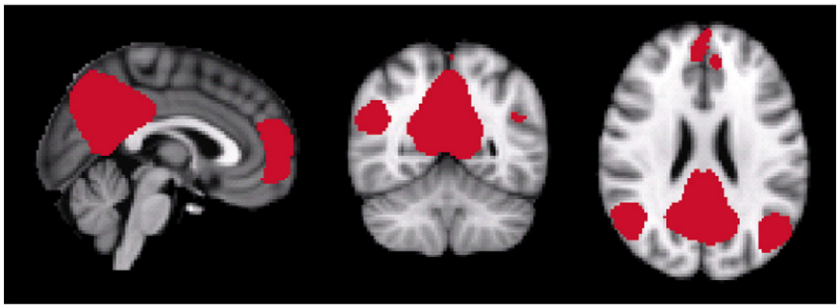

Fig. 2. DMN mask based on a group ICA shown in red. The regions shown ended up in a single component of a 30 component group ICA run. This includes the left and right MTL, Pc/PCC, MFC and left and right Inferior Parietal Cortex (IPC).

exception of the left and right MTL including hippocampi, were used as ROIs for every subsequent analysis. As described above, the hippocampi were replaced with a Freesurfer segmentation.

DMN parcellation

The preprocessed resting state fMRI data were used to parcellate the DMN of every subject, using the methods described above. An example of this parcellation is shown in Fig. 3, showing the Pc/PCC and MFC of subject 1. The parcellations of the other subjects are shown in the Supplementary materials. The colours were randomly assigned using the random-rainbow colour map from FSLView. This parcellation of the DMN regions divided them into a large number of sub-regions. Details on the number of regions and their size can be found in Tables 1 and 2. These sub-regions were used as a basis for a partial correlation analysis for each individual subject.

Resting state DMN connectivity

One graph based on resting state connectivity from the entire DMN was generated for each subject. These graphs contain information about the connectivity and organisation of the network. On the basis of the anatomical location of every node, any conclusion drawn from these graphs can be projected back onto the anatomy of the brain. These graphs were used to calculate the betweenness centrality for each sub-region of every subject, as described in the methods section. The resulting maps of average betweenness centrality are shown in Fig. 4. A related measure of connectivity, node degree, was also calculated and compared to the maps of betweenness centrality. The locations of the highest node degree and betweenness centrality match (figure shown in Supplementary materials), but the betweenness centrality provides a more spatially specific location with sharper edges of the hubs (Nijhuis et al., 2013), and was therefore used for all subsequent analysis. The betweenness centrality maps were transformed to z-scores and thresholded at $z > 1.7$ to define the resting state hubs. This analysis finds hubs in all the major regions of the DMN, except the left and right hippocampi. The betweenness centrality scores for these regions were not normally distributed, so a simple transformation to z-scores was not possible. The resulting hubs are shown in red in Fig. 5.

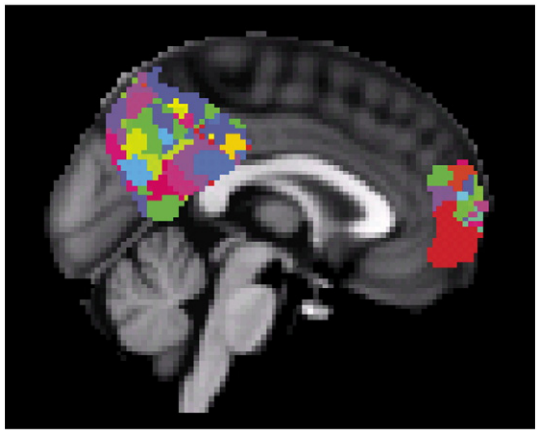

Fig. 3. Sub-regions of Pc/PCC and MFC of subject 1. The parcellations were created using single subject ICA results and resulted in an average of 61 sub-regions for the Pc/PCC and 21 for the MFC.

Diffusion DMN connectivity

Deterministic fibre tracts were obtained and inspected and compared to rs-fMRI results using Paraview[1]. The results for the combinations Pc/PCC-MFC, Pc/PCC-left MTL and Pc/PCC-right MTL are shown in Fig. 7. The DMN regions are shown in blue, resting state hubs in red, and fibre tracts in green. Fibre tracking results show a spatial match to the resting state hub results, meaning that the fibre tracts go through the spatial locations shown to be hubs in the resting state analysis. Figs. 8 and 9 show a detailed comparison of the resting state hubs in red, and the probabilistic tractography based connectivity in green and blue. The MFC and anterior Pc/PCC resting state hubs lie adjacent to the regions with high probabilistic tractography based connectivity, confirming the results from the deterministic tractography. Fig. 10 shows a 3D rendition of these same results, showing the close correspondence between the resting state hubs, and the probabilistic tractography results.

Discussion

This study utilises a combination of ICA and partial correlation analysis. ICA has become established over the years as a robust group analysis tool for rs-fMRI data (Beckmann et al., 2005; Comon, 1994; Kiviniemi, 2003; McKeown et al., 1998). The RSNs detected by ICA form networks that may be associated with distinct functional processes. Recently, the close correspondence between RSNs and functional regions was demonstrated (Smith et al., 2009). This further increases the confidence that ICA shows networks with an underlying functional relevance. This increased confidence forms the main motivation to use ICA to determine ROIs as a basis for network analysis. Previous work that this paper is based on involved partial correlation analysis using the AAL template as a basis to define ROIs (Salvador et al., 2005). However, for the present study there is no atlas available on the scale required. The ICA methods used in this work avoid this problem by determining the ROIs for the partial correlation analysis using single subject ICA results. This has the added benefit of not using group averages of large anatomical features, as is the case for the AAL template. The detailed size and shape of these structures vary between subjects, so even in a common space like MNI, some error is introduced in the

[1] http://www.paraview.org/.

Table 1
Average number of sub-regions across all subjects in the parcellation of the DMN. Standard deviation, smallest and largest number of sub-regions also included. Total number of regions is much larger than any atlas based method would provide, but low enough to allow the use of partial correlation coefficients.

	Number of sub-regions	SD	Min	Max
Complete DMN	122	18.6	68	152
Pc/PCC	61	10.8	33	83
MFC	21	5.2	9	32
RIPC	19	4.4	9	28
LIPC	24	5.0	14	36

Table 2
Average size of sub-regions in voxels across all subjects in the parcellation of the DMN. Standard deviation, smallest and largest size of sub-regions also included.

	Average size of regions (voxels)	SD	Min	Max
Complete DMN	97	143.3	1	2100
Pc/PCC	118	10.8	1	2100
MFC	74	117.1	1	1407
RIPC	67	93.2	1	857
LIPC	63	79.8	1	823

positioning, size and shape of the template ROIs. In this work, ROIs derived from the resting state data of the subjects themselves are used, rather than the gross anatomical average of some other group of subjects, and should hence be more closely related to the underlying functional organisation. Although to some degree the procedure used to resolve the overlapping regions is arbitrary, it is not expected to significantly impact the final result.

ICA based methods have been used previously to investigate the DMN in detail. Of particular interest is the recent work by Leech et al. (2012). They used ICA on Pc/PCC masked data to subdivide this region in smaller subregions, and investigate the connectivity of these regions with the rest of the brain. They found that various subregions of the Pc/PCC connect to different other RSNs. What is of particular interest is the subregions they found that connect the Pc/PCC to the rest of the DMN. If the hub results in Fig. 5 in this paper are compared with components 1 and 3 from Fig. 2a from the paper by Leech et al., it can be seen that the regions found are similar. Also of interest is the recent work by van den Heuvel and Sporns on the rich-club organisation of the structural connectivity of the human brain (van den Heuvel and Sporns, 2011). The rich-club nodes are essentially nodes which are central to the organisation of the connectome. This makes it very similar in concept to the betweenness centrality used in this work. The manner of presentation is different, but if the high-resolution connectome from van den Heuvel and Sporns is compared to the betweenness centrality hubs in this work, it does appear to be similar. Rich-club nodes appear to be in similar locations in the Pc/PCC to the betweenness centrality nodes.

As stated above, one main component method for this work is ICA. The other is partial correlation, which was performed on the time courses derived from the ICA parcellation. Partial correlation analysis is a well established method to examine functional connectivity in fMRI data. Correlational methods in general have been used since the start of the rs-fMRI field (Biswal et al., 1995; Lowe et al., 1998). They are used both to assess the functional connectivity between two ROIs, and to generate correlation maps of the brain based on a seed voxel. Partial correlation gives the additional benefit of identifying the unique connections between two regions with the contributions of all others 'partialled out'. This comes at the cost of needing more time points than ROIs to properly condition the sample covariance matrix that needs to be inverted. The combination of ICA and partial correlation forms a data driven technique, where the only user involvement required is the removal of noise and artefact components. Both of these methods benefit from long scanning times and a large number of data points.

This methodological approach has resulted in a detailed examination of the connectivity within the DMN. The analysis of the resulting functional connectivity yielded hubs of the DMN. The hubs found agree with previously published work on rs-fMRI hubs found for the entire brain (Tomasi and Volkow, 2011; van den Heuvel and Sporns, 2011; van den Heuvel et al., 2008a). They reside within the Pc/PCC, identified as a hub region for the DMN (Fransson and Marrelec, 2008; Hagmann et al., 2008). Of particular interest are the association areas that intersect with the DMN. When the hubs of the Pc/PCC DMN are compared to known anatomical information as shown in Fig. 6, the posterior hub matches the location of the HAA in the parieto-occipital sulcus, while the anterior hub is in the paralimbic association area (BA 23) (Achard et al., 2006; Mesulam, 1998; Nieuwenhuys et al., 2008). The hub of the MFL is also located in the paralimbic association area. See also Nieuwenhuys figures 12.3, 12.10, 12.13 and 15.47 (Nieuwenhuys et al., 2008). These two association areas are part of different large scale systems. The particular HAA shown in Fig. 6 is part of the parieto-occipital system, with BA23 and 32 being part of the paralimbic system. An association between HAAs and hubs in the brain has previously been reported by Bassett et al. (2008). This work however provides a much more specific spatial location to the hubs, which provides enough spatial specificity to resolve two different hubs related to two different large scale systems.

These HAAs are important to the functional organisation of the brain and DMN. For example, the PCC is strongly and reciprocally interconnected with many association areas. These include the Superior Parietal Lobule (SPL), the temporal polymodal cortex and the prefrontal lobe. These HAAs are mostly associated with the integration of multiple streams of information, which could be a plausible role for a hub region to fulfil. The location of the resting state hubs and diffusion based fibre termination points show a close match. The Pc/PCC–MFC fibre tracts from both the deterministic and the probabilistic analyses closely resemble the known anatomy of the cingulate bundle running from the frontal lobe directly towards the PCC. The fibre tracks running between SPL in Pc/PCC region and the MTL including the hippocampus are part of the parietotemporal HAA including the SPL, most of the IPL and a forwardly extending strip within the banks of the superior temporal sulcus in the temporal lobe (Nieuwenhuys et al., 2008). Although tractography

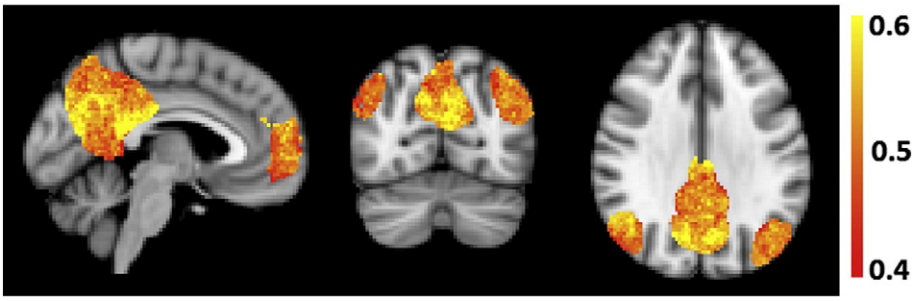

Fig. 4. Average betweenness centrality over all subjects.

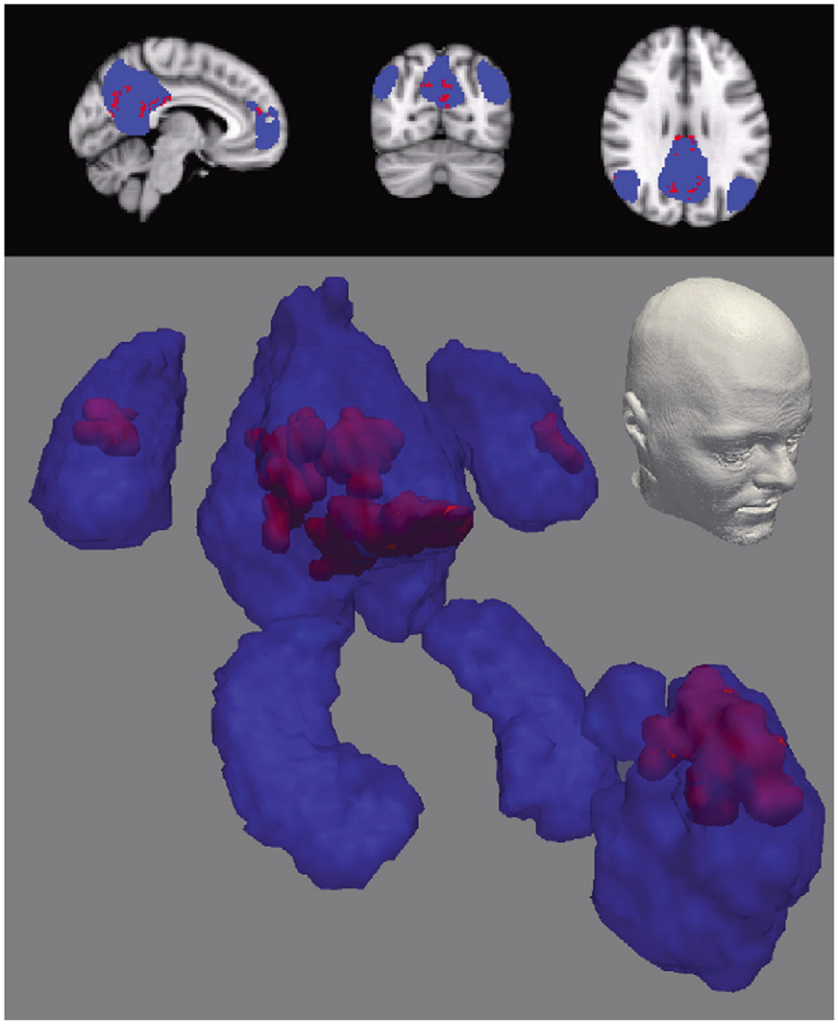

Fig. 5. Resting state DMN hubs shown in red, together with the DMN mask in blue. Top part of figure shows a 2D view using a sagittal, coronal and axial slice. Bottom part shows a 3D rendering of the DMN in blue, and the hubs in red. A rendering of a human head in the same orientation is added to show the point of view used.

only shows larger bundles of nerve fibres without giving information about their synapses, the tractography results of this study agree with studies in non-human primates which show that the parahippocampal gyrus of the MTL projects to the parts of the parietal cortex, the cingulate cortex and the MFC (van Hoesen, 1982). Hence this method may be of use in examining the detailed connectivity between two specific regions: details that can be missed when considering more global connectivity patterns. It also indicates that derived measures such as betweenness centrality can still show a good correlation with underlying measures of anatomical connectivity.

Both deterministic and probabilistic tractography were used in this work. Probabilistic tractography was added to compensate for any

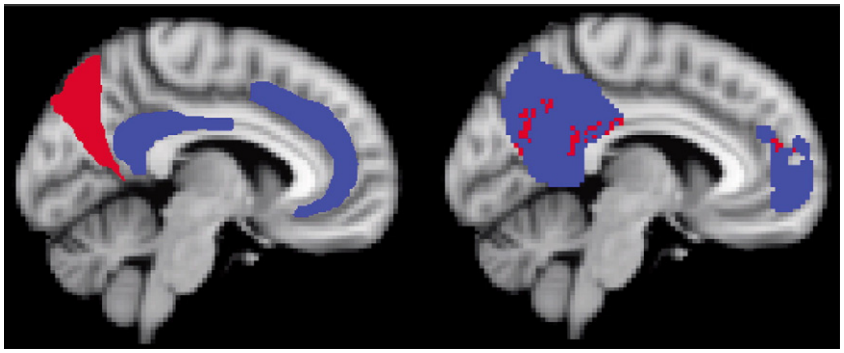

Fig. 6. Left: the association cortex as shown in Fig. 15.47B in Nieuwenhuys et al. (2008) is plotted on the medial view of an anatomical MRI scan. The red area indicates the heteromodal association area (HAA) of the parieto-occipital sulcus and the blue areas indicate part of the paralimbic association cortex (BA23 and BA32). Right: Hubs found using betweenness centrality. In this panel, blue shows the DMN, and red, the hubs. It can be seen that the hubs are located in the association areas as indicated in the left figure. Of the two hubs in the Pc/PCC of the DMN, one hub is located within the parieto-occipital HAA (red) and the other hub in the paralimbic association cortex (blue). The hub in the frontal lobe (BA32) is located in the paralimbic association cortex.

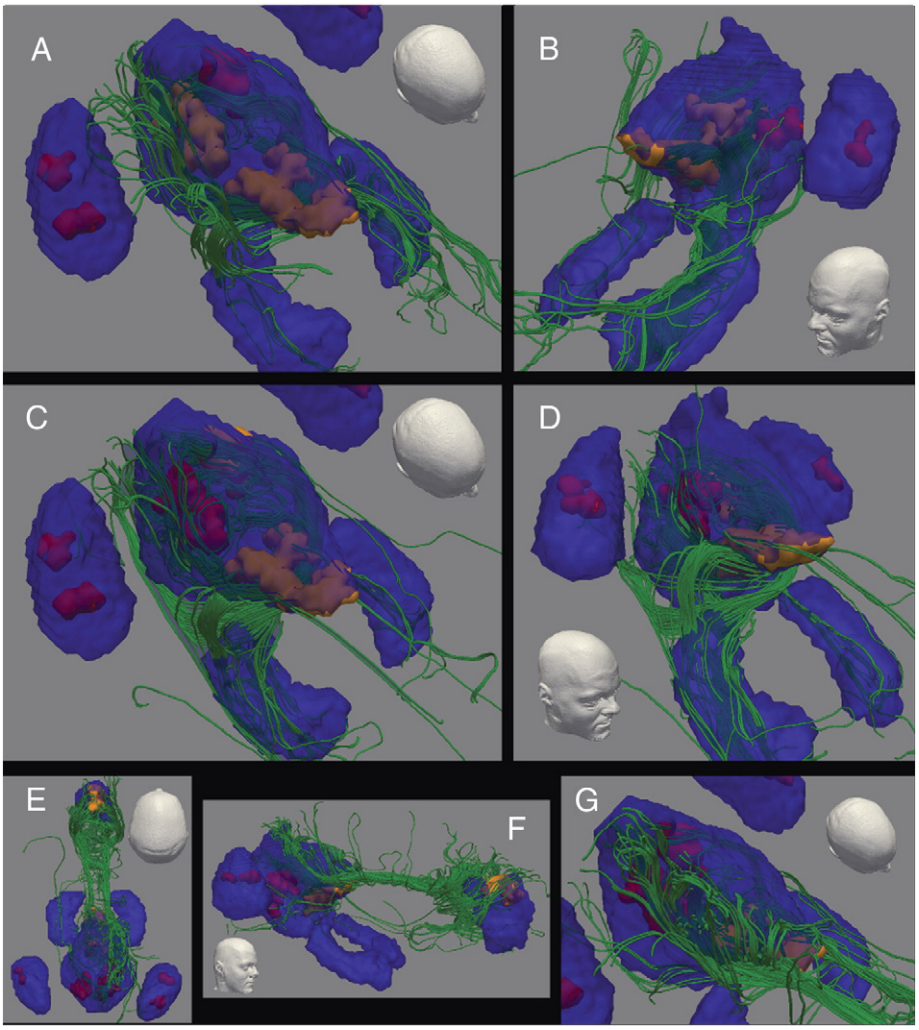

Fig. 7. Deterministic tractography results of the DMN, with the DMN ROIs in blue, rs-fMRI hubs in red/orange, and fibre tracts in green. Subfigures A/B, C/D and E/F/G show results for different combinations of DMN regions. Note that the hubs are shown through the transparent blue surface of the DMN, which can influence the hue of the red/orange of the underlying hubs. For each set, the hubs to which the fibre tracts connect are shown in orange. Subfigures A and B show 3D renderings of the results for the Pc/PCC and left MTL, C and D for the Pc/PCC and right MTL, and E, F and G for the combination of Pc/PCC and MFC. Each set of subfigures shows the same results as a 3D rendition, but rotated around to show the results from a different angle. A rendering of a human head in the same orientation is shown in each subfigure, to indicate the camera position. Fibre tracts in green are shown to track through the resting state hubs in orange. This shows the close match between the hubs, and the underlying anatomical connectivity.

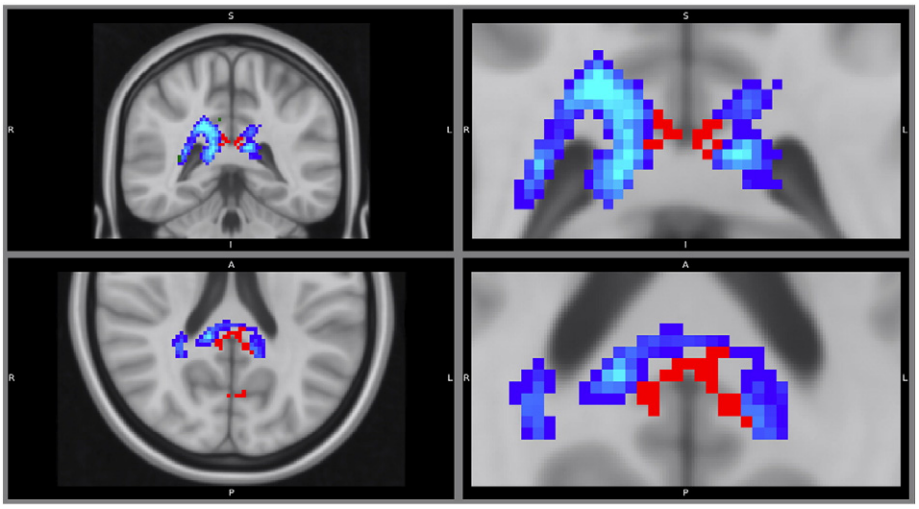

Fig. 8. Pc/PCC resting state hubs shown in red, probabilistic tractography results shown in blue. The regions with high tractography based connectivity lie adjacent to the anterior resting state hub, showing a close correspondence between the resting state and diffusion results.

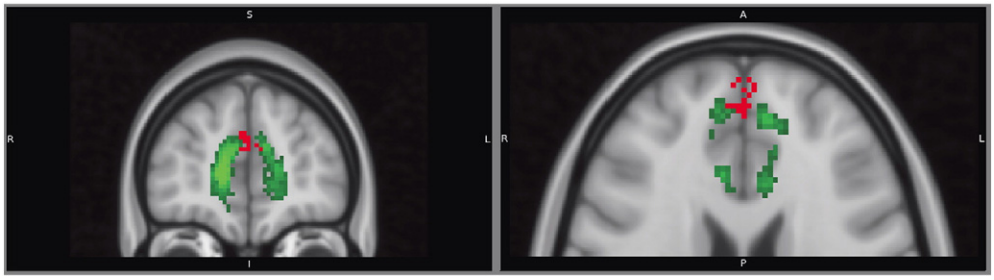

Fig. 9. MFC resting state hubs shown in red, probabilistic tractography results shown in green. The two results lie adjacent to each other, showing a close correspondence between the resting state and diffusion results.

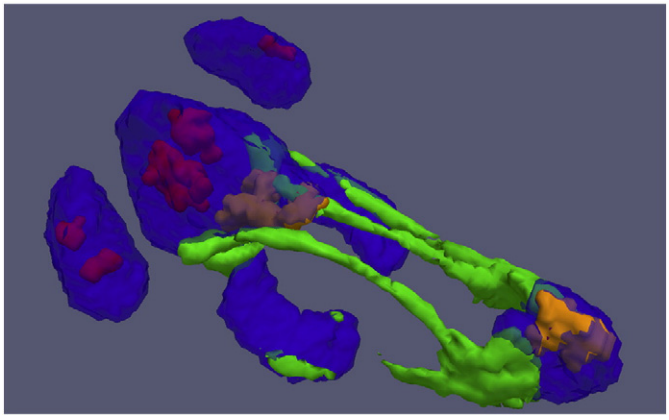

Fig. 10. 3D rendition of the DMN (blue), resting state hubs (red and orange) and probabilistic tractography results (green). The probabilistic tractography results confirm the deterministic tractography results shown in Fig. 7.

shortcomings in the older, simpler deterministic tractography. Results from both analyses were found to be comparable, with deterministic tracts lying within regions of high average fibre density. Previous work has already investigated the structural and functional organisation of the human brain. Where this work differs is the scale at which we investigate this organisation. The hub results from the functional analysis have a higher regional specificity than the large scale networks usually analysed. One example of the benefit of this specificity is shown in the separation of the hubs in the DMN belonging to different anatomical systems.

The data used for this project are all from healthy subjects. One interesting possibility for future research is to apply these methods to a patient group. For example, it has been shown that there are differences in DMN connectivity in ADHD patients vs. controls (Castellanos et al., 2008). Differences are also found in Alzheimer's disease (Greicius et al., 2004), autism (Kennedy and Courchesne, 2008) and schizophrenia (Bluhm et al., 2007). Examination of such patient groups can provide more information on the location of these connectivity changes. For example, the work by Bassett et al. showed a difference in the distribution of hubs in schizophrenia patients compared to healthy controls, when examining the brain on the scale of Brodmann's areas (Bassett et al., 2008).

In sum, using a novel combination of data driven techniques, we have presented an assessment of the resting state connectivity of the DMN on a finer scale than previously reported. Prominent findings include that hubs in the Precuneus/Posterior Cingulate Cortex and other regions for the DMN, correspond well to previously reported hubs of the entire brain, and to DTI fibre-tracking results of these same subjects. The locations of the hubs correspond with known heteromodal and paralimbic association areas, which are important for multi information integration.

Appendix A. Supplementary data

Supplementary data to this article can be found online at http://dx.doi.org/10.1016/j.neuroimage.2013.12.051.

References

Achard, S., Salvador, R., Whitcher, B., Suckling, J., Bullmore, E., 2006. A resilient, low-frequency, small-world human brain functional network with highly connected association cortical hubs. J. Neurosci. 26 (1), 63–72 (Jan.).

Bassett, D.S., Bullmore, E., Verchinski, B.A., Mattay, V.S., Weinberger, D.R., Meyer-Lindenberg, A., 2008. Hierarchical organization of human cortical networks in health and schizophrenia. J. Neurosci. 28 (37), 9239–9248 (Sep.).

Beckmann, C.F., Smith, S.M., 2004. Probabilistic independent component analysis for functional magnetic resonance imaging. IEEE Trans. Med. Imaging 23 (2), 137–152 (Feb.).

Beckmann, C.F., DeLuca, M., Devlin, J.T., Smith, S.M., 2005. Investigations into resting-state connectivity using independent component analysis. Phil. Trans. R. Soc. B Biol. Sci. 360 (1457), 1001–1013 (May).

Behrens, T., Woolrich, M., Jenkinson, M., Johansen-Berg, H., Nunes, R., Clare, S., Matthews, P., Brady, J., Smith, S., 2003. Characterization and propagation of uncertainty in diffusion-weighted MR imaging. Magn. Reson. Med. 50 (5), 1077–1088.

Behrens, T., Berg, H.J., Jbabdi, S., Rushworth, M., Woolrich, M., 2007. Probabilistic diffusion tractography with multiple fibre orientations: what can we gain? NeuroImage 34 (1), 144–155.

Biswal, B., Yetkin, F.Z., Haughton, V.M., Hyde, J.S., 1995. Functional connectivity in the motor cortex of resting human brain using echo-planar MRI. Magn. Reson. Med. 34 (4), 537–541 (Oct.).

Bluhm, R.L., Miller, J., Lanius, R.A., Osuch, E.A., Boksman, K., Neufeld, R.W.J., Théberge, J., Schaefer, B., Williamson, P., 2007. Spontaneous low-frequency fluctuations in the BOLD signal in schizophrenic patients: anomalies in the default network. Schizophr. Bull. 33 (4), 1004–1012 (Jul.).

Buckner, R.L., Andrews-Hanna, J.R., Schacter, D.L., 2008. The brain's default network: anatomy, function, and relevance to disease. Ann. N. Y. Acad. Sci. 1124, 1–38 (Mar.).

Castellanos, F.X., Margulies, D.S., Kelly, C., Uddin, L.Q., Ghaffari, M., Kirsch, A., Shaw, D., Shehzad, Z., Di Martino, A., Biswal, B., Sonuga-Barke, E.J.S., Rotrosen, J., Adler, L.A., Milham, M.P., 2008. Cingulate–precuneus interactions: a new locus of dysfunction

in adult attention-deficit//hyperactivity disorder. Biol. Psychiatry 63 (3), 332–337 (Feb.).
Cole, D.M., Smith, S.M., Beckmann, C.F., 2010. Advances and pitfalls in the analysis and interpretation of resting-state FMRI data. Front. Syst. Neurosci. 4, 8 (Jan., April).
Comon, P., 1994. Independent component analysis, A new concept? Signal Process. 36 (3), 287–314 (Apr.).
Cook, P.A., Bai, Y., Seunarine, K.K., Hall, M.G., Parker, G.J., Alexander, D.C., 2006. Camino: open-source diffusion-MRI reconstruction and processing. NeuroImage 14, 22858.
Cook, P.A., Symms, M., Boulby, P. a, Alexander, D.C., 2007. Optimal acquisition orders of diffusion-weighted MRI measurements. J. Magn. Reson. Imaging 25 (5), 1051–1058 (May).
Damoiseaux, J.S., Rombouts, S.a.R.B., Barkhof, F., Scheltens, P., Stam, C.J., Smith, S.M., Beckmann, C.F., 2006. Consistent resting-state networks across healthy subjects. Proc. Natl. Acad. Sci. 103 (37), 13848–13853 (Sep.).
Fox, M.D., Raichle, M.E., 2007. Spontaneous fluctuations in brain activity observed with functional magnetic resonance imaging. Nat. Rev. Neurosci. 8 (9), 700–711 (Sep.).
Fransson, P., Marrelec, G., 2008. The precuneus/posterior cingulate cortex plays a pivotal role in the default mode network: evidence from a partial correlation network analysis. NeuroImage 42 (3), 1178–1184 (Sep.).
Greicius, M.D., Krasnow, B., Reiss, A.L., Menon, V., 2003. Functional connectivity in the resting brain: a network analysis of the default mode hypothesis. Proc. Natl. Acad. Sci. 100 (1), 253–258 (Jan.).
Greicius, M.D., Srivastava, G., Reiss, A.L., Menon, V., 2004. Default-mode network activity distinguishes Alzheimer's disease from healthy aging: evidence from functional MRI. Proc. Natl. Acad. Sci. 101 (13), 4637–4642 (Mar.).
Greicius, M.D., Supekar, K., Menon, V., Dougherty, R.F., 2009. Resting-state functional connectivity reflects structural connectivity in the default mode network. Cereb. Cortex 19 (1), 72–78 (Jan.).
Hagmann, P., Cammoun, L., Gigandet, X., Meuli, R., Honey, C.J., Wedeen, V.J., Sporns, O., 2008. Mapping the structural core of human cerebral cortex. PLoS Biol. 6 (7), e159 (Jul.).
Kennedy, D.P., Courchesne, E., 2008. The intrinsic functional organization of the brain is altered in autism. NeuroImage 39 (4), 1877–1885 (Feb.).
Kiviniemi, V., 2003. Independent component analysis of nondeterministic fMRI signal sources. NeuroImage 19 (2), 253–260 (Jun.).
Kiviniemi, V., Starck, T., Remes, J., Long, X., Nikkinen, J., Haapea, M., Veijola, J., Moilanen, I., Isohanni, M., Zang, Y.-F., Tervonen, O., 2009. Functional segmentation of the brain cortex using high model order group PICA. Hum. Brain Mapp. 30 (12), 3865–3886 (Dec.).
Koch, M.A., Norris, D.G., Hund-Georgiadis, M., 2002. An investigation of functional and anatomical connectivity using magnetic resonance imaging. NeuroImage 16 (1), 241–250 (May).
Leech, R., Braga, R., Sharp, D.J., 2012. Echoes of the brain within the posterior cingulate cortex. J. Neurosci. 32 (1), 215–222 (Jan.).
Lowe, M.J., Mock, B.J., Sorenson, J.A., 1998. Functional connectivity in single and multislice echoplanar imaging using resting-state fluctuations. NeuroImage 7 (2), 119–132 (Feb.).
McKeown, M., Makeig, S., Brown, G., Jung, T.-P., 1998. Analysis of fMRI data by blind separation into independent spatial components. Hum. Brain Mapp. 6 (97), 160–188.
Mesulam, M.M., 1998. From sensation to cognition. Brain 121 (Pt 6), 1013–1052 (Jun.).
Nieuwenhuys, R., Voogd, J., Voogd, J., Huijzen, C., Huijzen, C., 2008. The Human Central Nervous System. Springer.
Nijhuis, E.H.J., van Cappellen van Walsum, A., Norris, D.G., 2013. Topographic hub maps of the human structural neocortical network. PLoS ONE 8 (6), e65511 (06).
Poser, B.A., Versluis, M.J., Hoogduin, J.M., Norris, D.G., 2006. BOLD contrast sensitivity enhancement and artifact reduction with multiecho EPI: parallel-acquired inhomogeneity-desensitized fMRI. Magn. Reson. Med. 55 (6), 1227–1235 (Jun.).
Raichle, M.E., Snyder, A.Z., 2007. A default mode of brain function: a brief history of an evolving idea. NeuroImage 37 (4), 1083–1090 (Oct., discussion 1097–9).
Raichle, M.E., MacLeod, A.M., Snyder, A.Z., Powers, W.J., Gusnard, D.A., Shulman, G.L., 2001. A default mode of brain function. Proc. Natl. Acad. Sci. 98 (2), 676–682 (Jan.).
Rubinov, M., Sporns, O., 2010. Complex network measures of brain connectivity: uses and interpretations. NeuroImage 52 (3), 1059–1069 (Sep.).
Salvador, R., Suckling, J., Coleman, M.R., Pickard, J.D., Menon, D., Bullmore, E., 2005. Neurophysiological architecture of functional magnetic resonance images of human brain. Cereb. Cortex 15 (9), 1332–1342 (Sep.).
Shulman, G.L., Fiez, J.A., Corbetta, M., Buckner, R.L., Miezin, F.M., Raichle, M.E., Petersen, S.E., 1997. Common blood flow changes across visual tasks: II. Decreases in cerebral cortex. J. Cogn. Neurosci. 9 (5), 648–663.
Skudlarski, P., Jagannathan, K., Calhoun, V.D., Hampson, M., Skudlarska, B.A., Pearlson, G., 2008. Measuring brain connectivity: diffusion tensor imaging validates resting state temporal correlations. NeuroImage 43 (3), 554–561 (Nov.).
Smith, S.M., Fox, P.T., Miller, K.L., Glahn, D.C., Fox, P.M., Mackay, C.E., Filippini, N., Watkins, K.E., Toro, R., Laird, A.R., Beckmann, C.F., 2009. Correspondence of the brain's functional architecture during activation and rest. Proc. Natl. Acad. Sci. 106 (31), 13040–13045 (Aug.).
Speck, O., Hennig, J., 1998. Functional imaging by I0- and T2*-parameter mapping using multi-image EPI. Magn. Reson. Med. 40 (2), 243–248 (Aug.).
Tomasi, D., Volkow, N.D., 2011. Functional connectivity hubs in the human brain. NeuroImage 57 (3), 908–917 (May).
Tuch, D.S., 2004. Q-ball imaging. Magn. Reson. Med. 52 (6), 1358–1372 (Dec.).
van den Heuvel, M.P., Hulshoff Pol, H.E., 2010. Specific somatotopic organization of functional connections of the primary motor network during resting state. Hum. Brain Mapp. 31 (4), 631–644 (Apr.).
van den Heuvel, M.P., Sporns, O., 2011. Rich-club organization of the human connectome. J. Neurosci. 31 (44), 15775–15786 (Nov.).
van den Heuvel, M., Mandl, R., Luigjes, J., Hulshoff Pol, H., 2008a. Microstructural organization of the cingulum tract and the level of default mode functional connectivity. J. Neurosci. 28 (43), 10844–10851 (Oct.).
van den Heuvel, M.P., Stam, C.J., Boersma, M., Hulshoff Pol, H.E., 2008b. Small-world and scale-free organization of voxel-based resting-state functional connectivity in the human brain. NeuroImage 43 (3), 528–539 (Nov.).
van den Heuvel, M.P., Kahn, R.S., Goni, J., Sporns, O., 2012. High-cost, high-capacity backbone for global brain communication. Proc. Natl. Acad. Sci. 109 (28), 11372–11377.
van Hoesen, G.W., 1982. The parahippocampal gyrus: new observations regarding its cortical connections in the monkey. Trends Neurosci. 5, 345–350.
Zwiers, M.P., 2010. Patching cardiac and head motion artefacts in diffusion-weighted images. NeuroImage 53 (2), 565–575 (Nov.).